# C-Terminal Region of Sulfite Reductase Is Important to Localize to Chloroplast Nucleoids in Land Plants

Yusuke Kobayashi, Takuto Otani, Kota Ishibashi, Toshiharu Shikanai, and Yoshiki Nishimura*

Laboratory of Plant Molecular Genetics, Department of Botany, Kyoto University, Japan

*Corresponding author: E-mail: yoshiki@pmg.bot.kyoto-u.ac.jp.

**Accepted:** April 18, 2016

## Abstract

Chloroplast (cp) DNA is compacted into cpDNA-protein complexes, called cp nucleoids. An abundant and extensively studied component of cp nucleoids is the bifunctional protein sulfite reductase (SiR). The preconceived role of SiR as the core cp nucleoid protein, however, is becoming less likely because of the recent findings that SiRs do not associate with cp nucleoids in some plant species, such as *Zea mays* and *Arabidopsis thaliana*. To address this discrepancy, we have performed a detailed phylogenetic analysis of SiRs, which shows that cp nucleoid-type SiRs share conserved C-terminally encoded peptides (CEPs). The CEPs are likely to form a bacterial ribbon–helix–helix DNA-binding motif, implying a potential role in attaching SiRs onto cp nucleoids. A proof-of-concept experiment was conducted by fusing the nonnucleoid-type SiR from *A. thaliana* (AtSiR) with the CEP from the cp nucleoid-type SiR of *Phaseolus vulgaris*. The addition of the CEP drastically altered the intra-cp localization of AtSiR to cp nucleoids. Our analysis supports the possible functions of CEPs in determining the localization of SiRs to cp nucleoids and illuminates a possible evolutionary scenario for SiR as a cp nucleoid protein.

**Key words:** nucleoid, sulfite reductase, evolution.

## Introduction

Plants originated from a eukaryotic ancestor that integrated a once free-living photosynthetic prokaryote closely related to present-day cyanobacteria, which led to the emergence of chloroplasts (cps; plastids) (Gray 1992; Timmis et al. 2004; Bowman et al. 2007; Bogorad 2008; Keeling 2010). Over time, a drastic transfer of genetic materials from the endosymbiont cyanobacteria (ancestral cps) to the eukaryotic host genome occurred. Consequently, only approximately 120–200 genes are encoded in cps (<10% of full-fledged cyanobacteria) (Timmis et al. 2004), although cpDNA and cp-encoded genes remain critical for photosynthesis, gene expression, and cp biogenesis (Allen 2003; Timmis et al. 2004; Stern et al. 2010).

cpDNA is packaged into cpDNA-protein complexes, called cp nucleoids (Kuroiwa 1991; Sakai et al. 2004; Pfalz and Pfannschmidt 2013, 2015; Powikrowska et al. 2014). Cp nucleoids can be visualized as dot-like structures in cps by staining with DNA-specific fluorochromes such as 4′,6-diamidino-2-phenylindole (DAPI) or SYBR Green I, and are ubiquitously observed in diverse taxa of plants and algae. Cp nucleoids are thought to be the functional unit of cpDNA replication, inheritance, and transcription (Kuroiwa 1991; Sakai et al. 2004; Pfalz and Pfannschmidt 2013, 2015; Powikrowska et al. 2014).

Several biochemical and proteomic analyses have revealed the composition of core cp nucleoid proteins (Yagi and Shiina 2012; Pfalz and Pfannschmidt 2013; Powikrowska et al. 2014). Thus far, bacterial histone-like proteins (Kobayashi et al. 2002; Karcher et al. 2009) and cp nucleoid SAP domain proteins (Kobayashi et al. 2016) have been reported as abundant components in cp nucleoids in unicellular algae. In land plants, various core cp nucleoid proteins have been reported, including sulfite reductase (SiR) (Sato et al. 2001; Chi-Ham et al. 2002), Whirly (Krupinska et al. 2014), SAP domain protein (Pfalz et al. 2006; Majeran et al. 2012) and Switch/sucrose nonfermentable complex B-4 (Melonek et al. 2012), whereas the *histone-like protein* gene has not been identified in any of the sequenced genomes. The different compositions of the cp nucleoid proteins could be attributed to cp nucleoid alterations during plant evolution, when the original prokaryotic components were lost or replaced by eukaryotic proteins (Kobayashi et al. 2016).

Among the cp nucleoid proteins, SiR was the first identified and has been extensively analyzed. SiR was identified as a

major component of the isolated cp nucleoids in soybean (*Glycine max*) (Cannon et al. 1999; Chi-Ham et al. 2002) and pea (*Pisum sativum*) (Sato et al. 1997, 2001), and it has the ability to compact DNA, and suppress DNA replication and transcription *in vitro* (Cannon et al. 1999; Sato et al. 2001; Sekine et al. 2007). SiR is a key enzyme for sulfur assimilation, catalyzing the reduction of sulfite to hydrogen sulfide and water using electrons via ferredoxins. In addition, recent studies indicated that SiR protects leaves against the toxicity of sulfite accumulation and prevents premature senescence caused by a greater sulfite accumulation (Yarmolinsky et al. 2013, 2014).

BLAST-based ortholog searches indicated that the amino acid sequence of SiR is highly conserved among virtually all plant species. Indeed, SiR was also identified in the cp nucleoids of a moss (*Physcomitrella patens*) (Wiedemann et al. 2010) and tobacco (*Nicotiana tabacum*) (Jeong et al. 2003). However, a growing number of reports have indicated that the SiR localization patterns are different among plant species. SiR was not identified in the cp nucleoids of *Zea mays* (Sekine et al. 2007; Majeran et al. 2012) or in the transcriptionally active chromosomes purified from *Arabidopsis thaliana* and mustard (Pfalz et al. 2006). Based on these reports, the previous assumption that SiR was a universal core cp nucleoid protein in land plants was an oversimplification.

To address this discrepancy, we phylogenetically analyzed SiR. A multiple sequence alignment analysis revealed that catalytic domains of SiRs are highly conserved, except for the C-terminal region. We found that nucleoid-type SiRs have conserved C-terminally encoded peptides (CEPs). The CEP in SiR was predicted to form a bacterial Ribbon–Helix–Helix DNA-binding motif and was not detected in the nonnucleoid-type SiRs in land plants, implying that it has an important role in the localization to cp nucleoids. We conducted an experiment to test our hypothesis by engineering *A. thaliana* SiR (AtSiR), which has been reported to localize in the stroma, free from cp nucleoids (Pfalz et al. 2006). Our analysis indicated the importance of the CEP in determining the localization of SiR to cp nucleoids and shed light on a possible evolutionary scenario for SiR as a cp nucleoid protein.

## Materials and Methods

### Multiple Sequence and Phylogenetic Analyses

SiR homologs were collected from searches using the BLAST algorithm against public databases. The sequences were aligned using ClustalW in MEGA 5.0 (Tamura et al. 2011). The full lengths of the SiR homologs were used for the phylogenetic analyses. Maximum parsimony- and maximum likelihood-based phylogenetic trees were constructed by MEGA 5.0 (Tamura et al. 2011). A Bayesian inference was performed using MrBayes version 3.2 (Ronquist et al. 2012). One million generations were completed, and trees were collected every 1,000 generations, after discarding trees corresponding to the first 25% (burn-in), to generate a consensus phylogenetic tree. Bayesian posterior probabilities were estimated as the proportion of trees sampled after burn-in.

### Homology Modeling

A homology model of the *P. sativum* SiR's CEP was constructed using Swiss Model using an *Escherichia coli* Transcriptional Repressor COPG/DNA complex homolog (Protein Data Bank: 1B01) as the template. All homology model images were produced using UCSF Chimera 1.5.3r.

### Vector Construction

Polymerase chain reaction (PCR) was performed using the proof-reading enzyme KOD-FX Neo (Toyobo Life Science, Osaka, Japan). The PCR products were separated using 1.2% agarose gel electrophoresis, and were gel-purified. AtSiR cDNA was amplified by primers 5′-CACCATGTCATCG ACGTTTCGAGCTCCG-3′ and 5′-TTGAGAAACTCCTTTGTA TGTA-3′. To generate *AtSiR-PvCEP*, overlapping PCR was performed. Briefly, PvCEP was amplified using primers 5′-TACAT ACAAAGGAGTTTCTCAACCATCACGCCACAATCTCAAGC-3′ and 5′-TTCACCTTTTCCATTTTGGTTG-3′. The PCR products of AtSiR and PvCEP were mixed and amplified using primers 5′-C ACCATGTCATCGACGTTTCGAGCTCCG-3′ and 5′-TTCACCTT TTCCATTTTGGTTG-3′. The resulting products were cloned into the pENTR/D-TOPO vector (Thermo Fisher Scientific Inc., Waltham, MA) and transferred into the pGWB41 vector (Nakagawa et al. 2007) using LR clonase (Thermo Fisher Scientific Inc.).

### Growth Conditions and Nuclear Transformations

*Arabidopsis thaliana* (Columbia) was grown in soil in a growth chamber (50 μmol of photons $m^{-2}$ $s^{-1}$, 16-h photoperiod, 23 °C). Nuclear transformation was performed using the Agrobacterium-mediated transformation method.

### Microscopic Observations

Confocal laser scanning microscopy of *A. thaliana* leaves was performed using a Leica TCS SP5 (Leica Microsystems, Wetzlar, Germany). To isolate cps, leaves were disrupted in 0.3 M mannitol medium using a surgical scalpel. Isolated cps were stained with 1 μg/ml DAPI and observed with an epifluorescence/differential interference microscope (BX51; Olympus, Tokyo, Japan) connected to a charge-coupled device camera (DP72; Olympus).

## Results and Discussions

### Nucleoid-Type SIRs Have Conserved Peptides in Their Termini

To reveal the molecular basis underlying the different localizations of SiRs in cps, their primary structures were compared

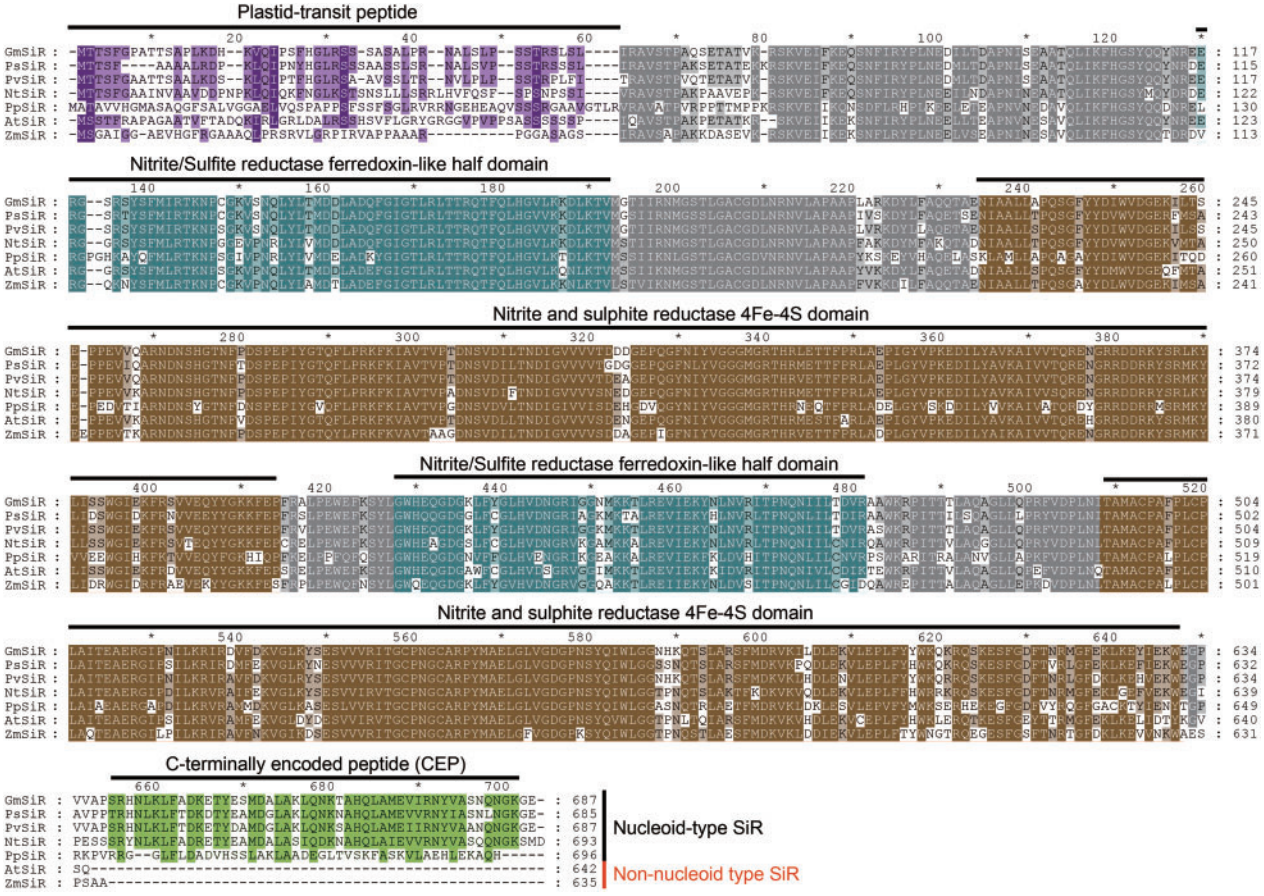


**Fig. 1.**—Multiple sequence alignment of SiRs in land plants. GmSiR, *Glycine max* SiR; PsSiR, *Pisum sativum* SiR; PvSiR, *Phaseolus vulgaris* SiR; NtSiR, *Nicotiana tabacum* SiR; AtSiR, *Arabidopsis thaliana* SiR; ZmSiR, *Zea mays* SiR.

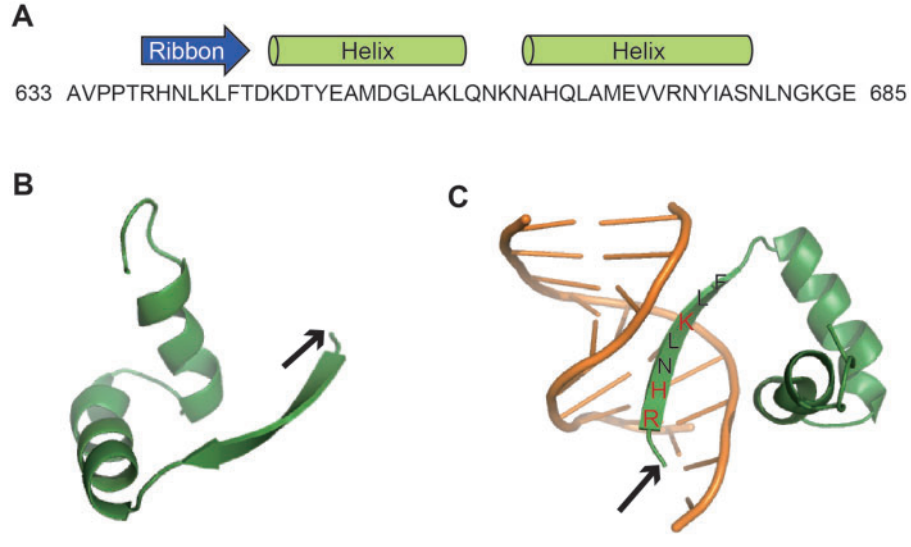


**Fig. 2.**—Homology model of the CEP in PsSiR. (*A*) C-terminal region of PsSiR. The blue arrow and green bar indicate the regions predicted to form Ribbon and Helix structures, respectively. (*B*) The homology model of the CEP in PsSiR was constructed using Swiss Model with an *E. coli* Transcriptional Repressor COPG homolog (Protein Data Bank: 1B01) as the template. CEP was predicted to form a bacterial Ribbon–Helix–Helix DNA-binding motif. The arrow indicates the N-terminus of the CEP. (*C*) Homology model of the CEP in PsSiR. The template was the *E. coli* Transcriptional Repressor COPG-homodimer/DNA complex (PDB: 1B01). Green indicates the PsCEP. The arrow indicates the N-terminus of the CEP. Red indicates basic amino acids.

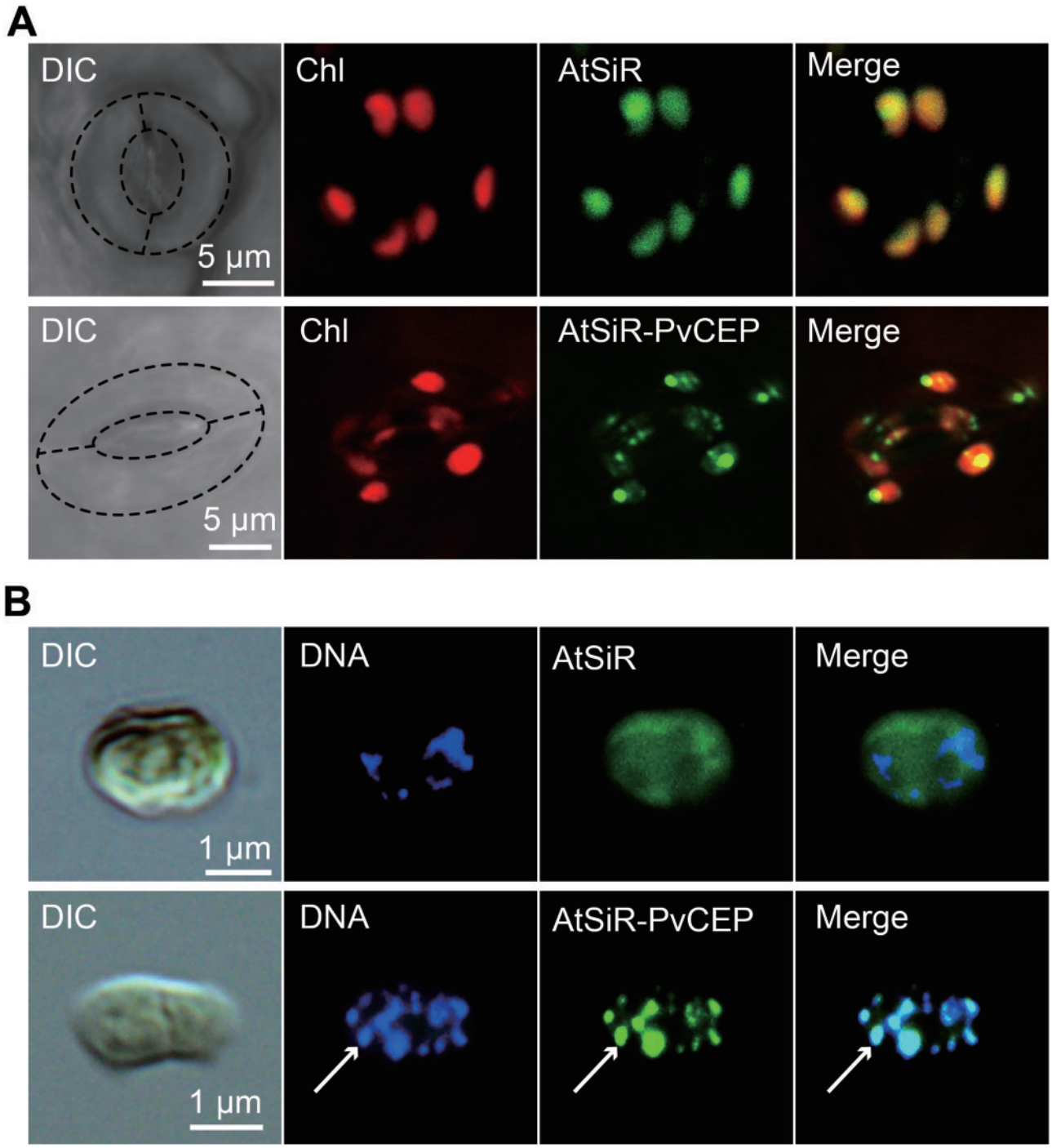


**Fig. 3.**—Localization of AtSiR and AtSiR-CEP. (*A*) Confocal microscopy of guard cells of *A. thaliana* expressing AtSiR-YFP or AtSiR-PvCEP-YFP under the control of the 35S promoter. Differential interference contrast microscopy shows the guard cells. Dot-lines trace the outline of the guard cells. Chl indicates the autofluorescence emitted by the chlorophyll. (*B*) Epifluorescence microscopy of cps isolated from *A. thaliana* expressing AtSiR-YFP or AtSiR-PvCEP-YFP under the control of the 35S promoter. Cps were stained with the DNA-specific fluorochrome DAPI. Arrows indicate a cp nucleoid.

using a multiple alignment analysis. Plant-type SiRs have two nitrite/SiR ferredoxin-like half domains (Pfam: 03460), and two nitrite and SiR 4Fe-4S domains (Pfam: 01077). Our sequence analysis showed that the catalytic domains are highly conserved in all plants, regardless of the localization patterns (fig. 1). However, a conserved short peptide (~50 amino acids) in the C-terminal region was found specifically in the amino acid sequences of cp nucleoid-type SiRs and not in the

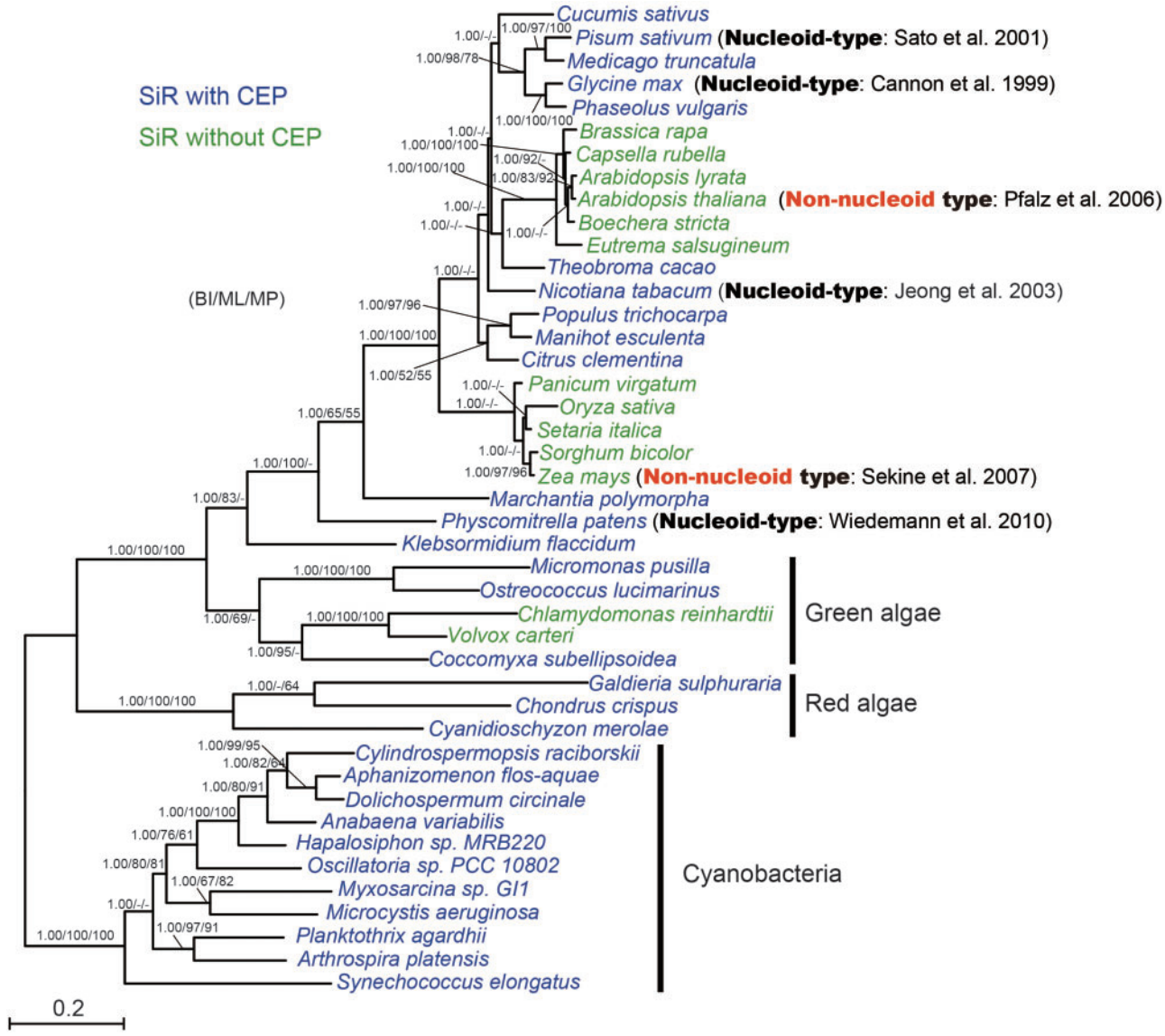


**Fig. 4.**—Phylogenetic points at which CEP was lost. A phylogenetic tree of SiRs based on Bayesian inference, maximum likelihood and maximum parsimony methods. Posterior probabilities for Bayesian inference (≥0.90) and Bootstrap values (≥50%) for the maximum likelihood and maximum parsimony, respectively, are indicated at the appropriate nodes. Blue indicates SiRs containing CEPs. Green indicates SiRs not containing CEPs.

nonnucleoid-type SiRs, such as *Z. mays*' SiR and AtSiR. The CEP was predicted to form a ribbon–helix–helix structure, a bacterial DNA-binding motif, using the SWISS homology modeling program (Biasini et al. 2014), suggesting that it has a role in attaching SiR onto cp nucleoids (fig. 2).

AtSiR was not identified in the transcriptionally active chromosomes purified from *Arabidopsis* and mustard chloroplasts, suggesting that AtSiR may not be specifically localized to cp nucleoids (Pfalz et al. 2006). To confirm the actual subcellular localization, a chimeric SiR protein fused with yellow fluorescent protein was expressed under the control of the 35S promoter (*35Sp::AtSiR-YFP*). Although the expression was driven by the constitutive promoter, the AtSiR-YFP fluorescence signal was mainly observed in the guard cells of independent stable lines (fig. 3*A*). This accumulation pattern is partly consistent with the transcriptome data, which indicated a relatively higher SiR expression level in guard cells than in mesophyll cells (Winter et al. 2007; Yang et al. 2008), implying a posttranscriptional regulation of *SiR* expression. A similar accumulation pattern was reported for the gene encoding ATP sulfurylase, the enzyme that catalyzes the entry step of the sulfate assimilation pathway (Bohrer et al. 2015). Confocal microscopy showed that AtSiR was localized uniformly in the chloroplast (fig. 3*A*). The DAPI staining of isolated cps

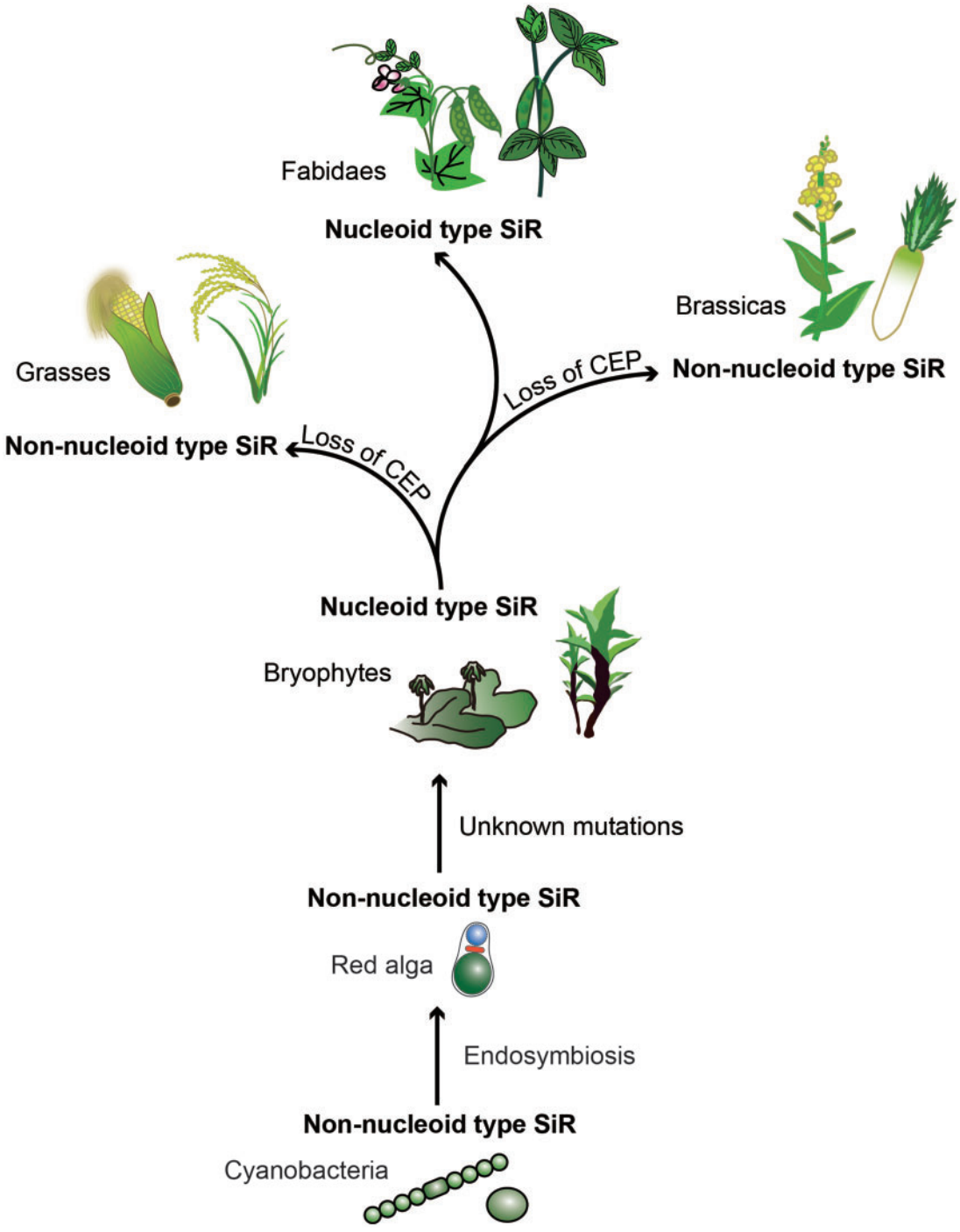


**Fig. 5.**—Schematic model representing the evolutionary history of the nucleoid-type SiR. Branch lengths do not represent phylogenetic distances.

showed that AtSiR-YFP is not preferentially colocalized with cp nucleoids, indicating that AtSiR is mainly localized to the stroma (fig. 3*B*).

We next tested whether the localization of AtSiR can be changed by the addition of CEP in cps. Chimeric AtSiR was fused with the CEP of the SiR from bean (*Phaseolus vulgaris*) and expressed under the control of the 35S promoter (*35Spro::AtSiR-PvSEP-YFP*). This chimeric protein was also mainly detected in the guard cells (fig. 3*A*). However, we found that the AtSiR-PvCEP-YFP fluorescence signals were observed as dot-like structures in cps (fig. 3*A*). DAPI staining of isolated cps showed that the AtSiR-PvCEP-YFP signal was

precisely co-localized with the cp nucleoids (fig. 3*B*). These results support our hypothesis that the CEP is a critical factor for SiR's binding to cp nucleoids.

### Evolution of SiRs as cp Nucleoid Protein

Bacterial SiR is a large enzyme with an α8β4 quaternary structure. The α-subunits contain both flavin adenine dinucleotide and flavin mononucleotide, whereas the β-subunits contain an iron-sulfur cluster coupled to a siroheme. The α-subunits have diaphorase activity that catalyzes the electron flow from NADPH to sulfite via flavin adenine dinucleotide, flavin mononucleotide and siroheme (Siegel and Davis 1974; Zeghouf et al. 2000). Plant- and cyanobacteria-type SiRs are homologous to the β-subunits and catalyze the reduction of sulfite using electrons donated from photosystem I via ferredoxin (Krueger and Siegel 1982). A previous biochemical analysis indicated that cyanobacterial SiR, which is thought to be the ancestor of chloroplast SiRs, is not localized to cp nucleoids (Sato et al. 2004)

To deduce the evolution of SiR as a cp nucleoid protein, a phylogenetic analysis was performed. One critical feature missing in nonnucleoid-type SiRs was CEP. CEP is conserved among plant SiRs, except for those in grasses and brassicas that do not colocalize with cp nucleoids (fig. 4), which implies that nonnucleoid-type SiRs in land plants could have been derived from cp nucleoid-type SiRs by the spontaneous loss of CEP. CEP is also detected in cyanobacterial SiRs and red algal SiRs. While the amino acid identities of cyanobacterial and red algal CEPs are relatively low when compared with those of land plants (e.g., the amino identity acid between *Cyanidioschyzon merolae* SiR [CmSiR] and PpCEP is <30%), these CEPs are also likely to form the RHH motif, suggesting that CEP originated from the endosymbiont's SiR (fig. 4, supplementary figs. S1 and S2, Supplementary Material online). We also found that CmSiR is closely related to cyanobacterial SiRs and distant from the cp nucleoid-type SiRs (fig. 4), which is consistent with CmSiR not localizing to cp nucleoids (Sato et al. 2004). Furthermore, SiRs in flowering plants showed close phylogenetic relationships regardless of the localization patterns (fig. 4). Thus, we propose that the evolution of nucleoid-type SiRs can be divided into three steps: First, ancient plant cells acquired the *SiR* gene from the endosymbiont cyanobacterium; Second, the SiR accumulated amino acid sequence changes, resulting in a conformational change that allowed the interaction with cp nucleoids prior to the birth of land plants; and finally, some land plants independently lost CEP, which is not essential for catalytic reactions, causing the conformational change that impaired their DNA-binding ability (fig. 5).

The physiological advantages of having SiR as a component of the cp nucleoids remain unclear. Plant SiR, which is regarded as the "bottleneck" in the reductive sulfate metabolic pathway (Khan et al. 2010), plays an important role in protecting leaves against the toxicity of sulfite accumulation. The protective function appears to be especially important in cps, because severe chlorophyll degradation, the reduction of D1 and psbO proteins, and the deterioration of photosynthesis were observed in SiR-impaired plants (Yarmolinsky et al. 2013, 2014). One possible physiological advantage of the association of SiR with cp nucleoids would be that SiR protects cpDNA from mutagenic bisulfite ion-based modifications (Sato et al. 2001) because cytosine can be converted to uracil by deamination when reacting with bisulfite (Clark et al. 1994). Another possibility is that the nucleoid-localized SiR acts as a sensor for the redox state within cps to modulate cp gene expression through the regulation of the cp nucleoid structure in response to various environmental conditions and developmental stages (Sekine et al. 2007).

We have not found any visible phenotypic effects caused by the overexpression of the cp nucleoid-type AtSiR-CEP in *A. thaliana* under normal growth conditions. However, the possibility remains that the association of SiR with cp nucleoids may be advantageous or disadvantageous under some conditions. Further analyses, including physiological and biochemical experiments, are necessary to reveal the functions of nucleoid-localized SiRs and why some land plants abandoned cp nucleoid-type SiRs during evolution.

## Supplementary Material

Supplementary figures S1 and S2 are available at *Genome Biology and Evolution* online (http://www.gbe.oxfordjournals.org/).

## Acknowledgments

The authors thank Dr Osami Misumi (Yamaguchi University) and Dr Naoki Sato (University of Tokyo) for their insightful and thoughtful advice. This work was supported, in part, by Ministry of Education, Culture, Sports, Science and Technology of Japan grants to T.S. and Y.N., the Core Stage Back-up Program from Kyoto University and Strategic Research Foundation Grant Aided-Project for Private Universities awarded to Y.N., the Funding Program for Next Generation World-Leading Researchers (NEXT Program: GS015), a Grant-in-Aid for Challenging Exploratory Research (26650111), a Grant for Basic Research Projects from the Sumitomo Foundation and a Grant-in-Aid for JSPS Fellows (grant 26·786 to Y.K.).

## Literature Cited

Allen JF. 2003. The function of genomes in bioenergetic organelles. Philos Trans R Soc Lond B Biol Sci. 358:19–37.

Biasini M, et al. 2014. SWISS-MODEL: modelling protein tertiary and quaternary structure using evolutionary information. Nucleic Acids Res. 42:W252–W258.

Bogorad L. 2008. Evolution of early eukaryotic cells: genomes, proteomes, and compartments. Photosynth Res. 95:11–21.

Bohrer A-S, et al. 2015. Alternative translational initiation of ATP sulfurylase underlying dual localization of sulfate assimilation pathways in plastids and cytosol in Arabidopsis thaliana. Front Plant Sci. 5:750.
Bowman JL, Floyd SK, Sakakibara K. 2007. Green genes-comparative genomics of the green branch of life. Cell 129:229–234.
Cannon GC, Ward LN, Case CI, Heinhorst S. 1999. The 68 kDa DNA compacting nucleoid protein from soybean chloroplasts inhibits DNA synthesis in vitro. Plant Mol Biol. 39:835–845.
Chi-Ham CL, Keaton MA, Cannon GC, Heinhorst S. 2002. The DNA-compacting protein DCP68 from soybean chloroplasts is ferredoxin: sulfite reductase and co-localizes with the organellar nucleoid. Plant Mol Biol. 49:621–631.
Clark SJ, Harrison J, Paul CL, Frommer M. 1994. High sensitivity mapping of methylated cytosines. Nucleic Acids Res. 22:2990–2997.
Gray MW. 1992. The endosymbiont hypothesis revisited. Int Rev Cytol. 141:233–357.
Jeong SY, Rose A, Meier I. 2003. MFP1 is a thylakoid-associated, nucleoid-binding protein with a coiled-coil structure. Nucleic Acids Res. 31:5175–5185.
Karcher D, Koster D, Schadach A, Klevesath A, Bock R. 2009. The Chlamydomonas chloroplast HLP protein is required for nucleoid organization and genome maintenance. Mol Plant. 2:1223–1232.
Keeling PJ. 2010. The endosymbiotic origin, diversification and fate of plastids. Philos Trans R Soc Lond B Biol Sci. 365:729–748.
Khan MS, et al. 2010. Sulfite reductase defines a newly discovered bottleneck for assimilatory sulfate reduction and is essential for growth and development in *Arabidopsis thaliana*. Plant Cell 22:1216–1231.
Kobayashi T, et al. 2002. Detection and localization of a chloroplast-encoded HU-like protein that organizes chloroplast nucleoids. Plant Cell 14:1579–1589.
Kobayashi Y, et al. 2016. Eukaryotic components remodeled chloroplast nucleoid organization during the green plant evolution. Genome Biol Evol. 8:1–16.
Krueger RJ, Siegel LM. 1982. Spinach siroheme enzymes: isolation and characterization of ferredoxin-sulfite reductase and comparison of properties with ferredoxin-nitrite reductase. Biochemistry 21:2892–2904.
Krupinska K, et al. 2014. WHIRLY1 is a major organizer of chloroplast nucleoids. Front Plant Sci. 5:432.
Kuroiwa T. 1991. The replication, differentiation, and inheritance of plastids with emphasis on the concept of organelle nuclei. Int Rev Cytol. 128:1–62.
Majeran W, et al. 2012. Nucleoid-enriched proteomes in developing plastids and chloroplasts from maize leaves: a new conceptual framework for nucleoid functions. Plant Physiol. 158:156–189.
Melonek J, Matros A, Trosch M, Mock HP, Krupinska K. 2012. The core of chloroplast nucleoids contains architectural SWIB domain proteins. Plant Cell 24:3060–3073.
Nakagawa T, et al. 2007. Development of series of gateway binary vectors, pGWBs, for realizing efficient construction of fusion genes for plant transformation. J Biosci Bioeng. 104:34–41.
Pfalz J, Liere K, Kandlbinder A, Dietz KJ, Oelmuller R. 2006. pTAC2, -6, and -12 are components of the transcriptionally active plastid chromosome that are required for plastid gene expression. Plant Cell 18:176–197.
Pfalz J, Pfannschmidt T. 2013. Essential nucleoid proteins in early chloroplast development. Trends Plant Sci. 18:186–194.
Pfalz J, Pfannschmidt T. 2015. Plastid nucleoids: evolutionary reconstruction of a DNA/protein structure with prokaryotic ancestry. Front Plant Sci. 6:220.
Powikrowska M, Oetke S, Jensen PE, Krupinska K. 2014. Dynamic composition, shaping and organization of plastid nucleoids. Front Plant Sci. 5:424.
Ronquist F, et al. 2012. MrBayes 3.2: efficient Bayesian phylogenetic inference and model choice across a large model space. Syst Biol. 61:539–542.
Sakai A, Takano H, Kuroiwa T. 2004. Organelle nuclei in higher plants: structure, composition, function, and evolution. Int Rev Cytol. 238:59–118.
Sato N, et al. 2004. Discontinuous evolution of plastid genomic machinery: radical replacement of major DNA-binding proteins. Endocytobiosis Cell Res. 15:286–293.
Sato N, Misumi O, Shinada Y, Sasaki M, Yoine M. 1997. Dynamics of localization and protein composition of plastid nucleoids in light-grown pea seedlings. Protoplasma 200:163–173.
Sato N, Nakayama M, Hase T. 2001. The 70-kDa major DNA-compacting protein of the chloroplast nucleoid is sulfite reductase. FEBS Lett. 487:347–350.
Sekine K, et al. 2007. DNA binding and partial nucleoid localization of the chloroplast stromal enzyme ferredoxin: sulfite reductase. FEBS J. 274:2054–2069.
Siegel LM, Davis PS. 1974. Reduced nicotinamide adenine dinucleotide phosphate-sulfite reductase of enterobacteria. IV. The *Escherichia coli* hemoflavoprotein: subunit structure and dissociation into hemoprotein and flavoprotein components. J Biol Chem. 249:1587–1598.
Stern DB, Goldschmidt-Clermont M, Hanson MR. 2010. Chloroplast RNA metabolism. Annu Rev Plant Biol. 61:125–155.
Tamura K, et al. 2011. MEGA5: molecular evolutionary genetics analysis using maximum likelihood, evolutionary distance, and maximum parsimony methods. Mol Biol Evol. 28:2731–2739.
Timmis JN, Ayliffe MA, Huang CY, Martin W. 2004. Endosymbiotic gene transfer: organelle genomes forge eukaryotic chromosomes. Nat Rev Genet. 5:123–135.
Wiedemann G, et al. 2010. Targeted knock-out of a gene encoding sulfite reductase in the moss *Physcomitrella patens* affects gametophytic and sporophytic development. FEBS Lett. 584:2271–2278.
Winter D, et al. 2007. An "Electronic Fluorescent Pictograph" browser for exploring and analyzing large-scale biological data sets. PLoS One 2:e718.
Yagi Y, Shiina T. 2012. Evolutionary aspects of plastid proteins involved in transcription: the transcription of a tiny genome is mediated by a complicated machinery. Transcription 3:290–294.
Yang Y, Costa A, Leonhardt N, Siegel RS, Schroeder JI. 2008. Isolation of a strong *Arabidopsis* guard cell promoter and its potential as a research tool. Plant Methods 4:1746–1746.
Yarmolinsky D, Brychkova G, Fluhr R, Sagi M. 2013. Sulfite reductase protects plants against sulfite toxicity. Plant Physiol. 161:725–743.
Yarmolinsky D, et al. 2014. Impairment in sulfite reductase leads to early leaf senescence in tomato plants. Plant Physiol. 165:1505–1520.
Zeghouf M, Fontecave M, Coves J. 2000. A simplifed functional version of the *Escherichia coli* sulfite reductase. J Biol Chem. 275:37651–37656.

**Associate editor:** Bill Martin